





---

# DETECTION TRANSFORMERS UNDER THE KNIFE: A NEUROSCIENCE-INSPIRED APPROACH TO ABLATIONS

---

 Nils Hütten\*,  Florian Hölken,  Hasan Tercan,  Tobias Meisen  
 Institute for Technologies and Management of Digital Transformation (TMDT)  
 University of Wuppertal  
 Rainer Gruenter Str. 21, 42119, Wuppertal, Germany

## ABSTRACT

In recent years, explainable artificial intelligence (XAI) has gained traction as an approach to enhancing model interpretability and transparency, particularly in complex models such as detection transformers. Despite rapid advancements, a substantial research gap remains in understanding the distinct roles of internal components - knowledge that is essential for improving transparency and efficiency. Inspired by neuroscientific ablation studies, which investigate the functions of brain regions through selective impairment, we systematically analyze the impact of ablating key components in three state-of-the-art detection transformer models: detection transformer (DETR), deformable detection transformer (DDETR), and DETR with improved denoising anchor boxes (DINO). The ablations target query embeddings (QEs), encoder and decoder Multi-head self-attention (MHSA) as well as decoder Multi-head cross-attention (MHCA) layers. We evaluate the consequences of these ablations on the performance metrics generalized intersection over union (gIoU) and F1-score, quantifying effects on both the classification and regression sub-tasks on the COCO dataset. To facilitate reproducibility and future research, we publicly release the DeepDissect library.

Our findings reveal model-specific resilience patterns: while DETR is particularly sensitive to ablations in encoder MHSA and decoder MHCA, DDETR's multi-scale deformable attention enhances robustness, and DINO exhibits the greatest resilience due to its look-forward twice update rule, which helps distributing knowledge across blocks. These insights also expose structural redundancies, particularly in DDETR's and DINO's decoder MHCA layers, highlighting opportunities for model simplification without sacrificing performance. This study advances XAI for detection transformers by clarifying the contributions of internal components to model performance, offering insights to optimize and improve transparency and efficiency in critical applications.

**Keywords** Explainable AI · Ablation Study · Computer Vision · Object Detection · Detection Transformer · Neuroscience

## 1 Introduction

The advent of deep learning has revolutionized computer vision, with convolutional neural networks (CNNs) advancing tasks like classification, object detection, and segmentation. More recently, vision transformers (VTs) have emerged, leveraging attention mechanisms to handle long-range dependencies in image data [1, 2]. Originally developed for sequence tasks, transformers now rival or outperform CNNs in visual benchmarks [3, 4], driving rapid adoption in both academia and industry [5, 6]. The pursuit of benchmark performance and inference times, drives increasing model complexity, as seen in the evolution of models such as BERT [7], GPT [8], LLAMA, and VT models like ViT, Swin, or Focal Transformer [4] [2, 9, 10, 11, 12]. Despite their success, these models pose significant challenges regarding explainability and interpretability. Although XAI is an active field, specific investigations into VTs remain limited [13, 14, 15]. In particular, methodology to reveal how knowledge acquired during training is internally represented remains underexplored [5], yet is crucial for building transparent and trustworthy models, especially in high-stakes domains like autonomous driving and medical diagnosis.

---

\*Corresponding author. *E-mail address*: Nhuetten@Uni-Wuppertal.de

The field of neuroscience offers valuable inspiration for addressing this gap. Techniques like ablative brain surgery—selective removal of neural tissue—have been instrumental in identifying brain regions responsible for specific cognitive and motor functions [16, 17, 18, 19]. Inspired by this, early studies by Meyes et al. [20] applied neuroscientifically inspired ablations (NIAs) to simple multi-layer perceptrons (MLPs) and CNNs to enhance interpretability.

In our work, we extend this approach to modern VTs to address key challenges in XAI for object detection. Traditional XAI methods - such as feature attribution and gradient-based techniques - primarily focus on identifying influential input regions, yet often fail to provide insights into the internal structure and functional roles of model components. In contrast, NIA studies offer a systematic way to isolate and analyze their contributions individually, shedding light on how knowledge is represented and utilized within the network. We adapt this methodology to address our central research question "How do architectural developments in detection transformers affect the internal organization of learned representations with respect to the regression and classification subtask?". Our contributions are twofold. First, we provide new insights into the knowledge distribution and the performance contributions of key architectural components by conducting NIA studies on three key VT models for object detection. Second, we release the Python-based library *DeepDissect*, which facilitates the execution of NIA studies on models within the MMDetection [21] framework.

Using *DeepDissect* we carried out a systematic ablation study across three architectures from the detection transformer family, focusing on key model components like acqes and encoder/decoder projection matrices. For each component, we performed full layer ablations, from 5-50%, as well as block-wise ablation with a constant ablation level of 30%. The models were evaluated on the common objects in context (COCO) validation set [22] using both classification and regression metrics to quantify the impact of the ablations on performance. Our results provide a deeper understanding of how knowledge is represented within DETR models, offering insights into the internal semantics of their components and how each contributes to the models' overall functionality. By identifying the contribution and actual function of each component, we pave the way for optimizing these architectures, for more efficiency and interpretability.

## 2 Related Work

The term *ablation* in the context of technical systems was originally introduced by Newell [23] as a method for analyzing the contribution of individual components by removing them and observing the resulting changes in system performance. He argued that, in complex systems composed of modular knowledge sources, ablation could reveal valuable insights about the internal structure and function. Even in deliberately engineered systems, the specific contributions of individual parts are not always well understood, making ablation a pragmatic tool for analyzing internal structure and functional contributions. This principle remains relevant for modern artificial neural networks (ANNs), where internal mechanisms often remain opaque despite careful design.

In deep learning, ablation studies have evolved into a widely used but broadly defined methodological category. The term is often applied to a wide range of experiments aimed at demonstrating improvements in performance or efficiency. These include hyperparameter tuning (e.g., ResNeXt, Faster R-CNN, FPN, and DETR [24, 25, 26, 27]), structural modifications such as the omission or replacement of components (e.g., RCNN, Faster R-CNN and DETR [28, 25, 27]), and interventions on information pathways (notably in FPN and DETR [26, 27]). Additionally, studies like Hameed et al. [29] examine input-level ablations through image perturbation. These experiments are typically conducted pre-training, but also rarely are done post-training. Further, while all these approaches are commonly labeled as ablation studies, they are often conducted to retrospectively justify design choices—demonstrating that a newly introduced module or mechanism yields a measurable benefit, rather than to gain insight into the model's internal structure per se.

However, an alternative perspective, inspired by neuroscience regards ablations as a means for improving model interpretability rather than solely measuring performance. The concept of NIA involves disabling trainable weights by setting them to zero in a trained ANN to block signal flow. Pioneering work in this direction by Meyes et al. [20] examined the performance of a MLP and a VGG-19 CNN trained on the classification datasets MNIST and ImageNet, respectively. Their findings revealed that certain MLP units or CNN layers play a disproportionately substantial role in determining the overall outcome, either by representing general concepts or class-specific features. These insights were generalized by Vishnusai et al. [30] through NIA studies with different models trained on MNIST. Lilian et al. [31] extended the approach to robot control based on reinforcement learning, demonstrating that ANN exhibit a degree of logical organization, in addition to resilience to structural damage.

Furthermore, the blackbox nature of ANN can be further addressed by combining ablations with methods such as gradient weighted class activation mappings (Grad-CAM) [32]. For example, the transparency and interpretability of a one-dimensional CNN used for failure prediction in industrial sensor data were improved by demonstrating that its learned filters aligned with Grad-CAM explanations and were intuitively understandable to domain experts [33]. While methods like Grad-CAM highlight relevant input regions by mapping model decisions back to input features, ablation

studies offer a complementary perspective: they probe the internal structure of the model by selectively disabling components, thereby revealing how specific internal representations contribute to overall function.

While the model compression technique *pruning* often employs similar experimental setups, their underlying motivation fundamentally differs from that of NIA studies. Recent applications of pruning enabled natural language processing (NLP) models like SparseGPT [34], ShortGPT [35], Wanda [36], UPop [37] and Shortened LLaMa [38]. There have also been pruning endeavours on VT models like shifted window transformer (Swin), ViT [39, 40, 41] and also DETR models [42, 43]. The primary goal of pruning is to reduce model size and computational cost, and it usually does not distinguish between pruned parameters at the component level. Furthermore, most methods introduce additional learnable components to determine which (partial) network structures are to be excluded, making them unsuitable for XAI purposes. Hence, due to the fundamentally different objectives and level of detail of assessments, meaningful comparisons between NIA studies and pruning are not adequate.

### 3 Methodology

Guided by our aforementioned key research question, we conduct a structured NIA study across three key DETR-based architectures, all trained on the COCO dataset. These models represent significant advancements in detection transformer technology: the original DETR [27], DDETR [44], and DINO [45]. DDETR introduced two new architectural features: deformable attention layers and multi-scale feature processing. Deformable attention reduces computational cost by attending only to a set of  $k$  predicted offsets with regard to a reference point per attention head. These reference points are an additional input to the first decoder block and are defined and optimized the same way as QEs. The multiscale features are extracted from different layers in the ResNet-50 backbone and jointly used as the input for the encoder MHSA. Although DDETR also explores bounding box refinement via dynamic priors and two-stage architectures, we exclude these variants to keep the scope of the study manageable and to maintain a certain architectural difference to DINO. DINO introduced three novel concepts: contrastive denoising training to reduce duplicate detections; mixed query selection fusing encoder outputs with QEs; and the look-forward twice update rule to achieve faster convergence through an additional gradient path in neighboring decoder blocks.

To systematically investigate the models, we designed a set of coherent ablation studies grounded in the base DETR architecture for consistency. In this regard, it seemed logical to focus on the components that distinguish DETR from CNNs and NLP transformers: MHSA/MHCA layers, learnable QEs forming the decoder input, and additional auxiliary loss terms to stabilize training.

We decided to ablate the input projection matrices ( $W_q, W_k, W_v$ ) of the encoder MHSA, decoder MHSA, and decoder MHCA since these directly impact the attention computation. The first set of ablation studies is conducted simultaneously across all transformer blocks, removing 5%, 15%, 30%, and 50% of the weights, referred to as *full ablations*. Additional *block-wise ablations* consider the distribution of learned representations across transformer blocks, targeting the desired component in one block at a time. They were conducted only on the attention layers at 30%, due to the significance of the effect in full ablations and resource constraints. We perform ablations by randomly zeroing the specified percentage of weights within the targeted component, effectively blocking signal flow. We then evaluate the model on the validation set, comparing its performance against the unmodified state (see Fig. 1). Each experiment includes 100 random configurations per ablation level, chosen to balance statistical robustness and computational efficiency (see Appendix Fig. A1 for variance stabilization trends).

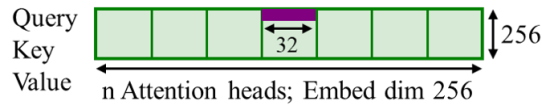


Figure 1: Visualization of multi-head attention ablations on  $1 \times 32$  subunits representing attention heads in projection matrices.

QEs are ablated individually, at the scalar level. For the multi-head attention components we ablate  $1 \times 32$  vectors from projection matrices, preserving the coherence of subunits within the attention mechanism (Fig. 1, right). To discern whether the classification and regression aspects of the object detection task are organized within specific model regions or evenly distributed, we apply two distinct metrics and bounding box matching approaches. For classification performance, we use the F1-score, while regression performance is evaluated with the gIoU [46]. To calculate the F1-score, we first match the predicted bounding boxes with the corresponding ground truth boxes based on the gIoU via the Hungarian algorithm. After excluding unmatched or invalid detections, the scores are determined using a weighted

average across classes, which considers the varying instance counts per class, yielding an overall metric that accurately reflects the model’s classification performance across the entire dataset.

The gIoU adjusts the intersection over union (IoU) by incorporating the area of the smallest enclosing box containing prediction and ground truth, which quantifies regression accuracy even for bounding boxes that do not overlap with the ground truth, offering a more comprehensive assessment of spatial alignment. This adjustment penalizes predictions that are distant from the ground truth, providing a more robust measure of localization accuracy. To obtain an overall metric, we compute the weighted average across classes, giving us the mean generalized intersection over union (mgIoU).

## 4 Results & Analysis

In this section, we formulate hypotheses based on the original publications introducing the respective models and examine them in light of our ablation study results. As baselines, we use models trained on the COCO dataset, provided by MMDetection [21]. Their performances are summarized in tab. 1. The baseline results highlight the progress in regression performance across the three models - from DETR to DDETR and finally DINO. Interestingly, classification performances remains largely stable across models, with DETR and DDETR even slightly outperforming the more recent DINO model in this sub-task.

Model	mgIoU (%)	F1-score (%)
<b>DETR</b>	70.35	85.17
<b>DDETR</b>	73.99	85.67
<b>DINO</b>	81.27	84.88

Table 1: Baseline performance of models in terms of mgIoU and F1-score.

### 4.1 Detection Transformer Model (DETR)

The initial DETR paper presented ablation experiments that are typical for the introduction of new models. These included variations in the number of encoder and decoder blocks, removal of feed forward networks (FFN), and different configurations for spatial positional encodings. Removing all encoder blocks resulted in a performance drop of 3.9 %p in mean average precision (mAP), while using predictions from the first decoder block instead of the last led to a more substantial reduction of 8.2%p. The newly introduced QEs were considered indispensable by the authors, so only the spatial position encodings were removed or their entryptpoint into the model was changed. This led to a maximum reduction in mAP of 7.8%p upon removal. In contrast to our experiments, these modifications were applied prior to training, but still can serve as a sound basis for forming our hypotheses. Based on these results, we expect a continuous decline of mgIoU and F1-score for the full ablations with increasing ablation percentage, with decoder attention being most sensitive, followed by QEs and finally encoder MHSA. We cannot derive any assumptions from the initial experiments by Carion et al. delineating classification from regression performance, but based on the characteristics of the metrics, regression should be more susceptible than classification, given its direct connection to localization errors. For the block-wise ablations, we expect a continuously increasing performance reduction the deeper the ablated block. In the case of the decoder, this would be consistent with the original paper. For the encoder, it aligns with the widely accepted notion that features become increasingly refined—and therefore more critical to function—the deeper they are processed within the network. Figure 2 illustrates the performance differences resulting from the NIAs, with gIoU shown as dot markers on solid lines and F1-score as cross markers on dashed lines. The x-axis indicates ablation percentages, and each plot is labeled with the corresponding model component. Contrary to our hypothesis, ablating the decoder MHSA had minimal impact on regression and even slightly improved classification at higher ablation levels. It appears that the re-projection of the queries is not required in the fully trained state, as the information provided to the decoder MHCA layer by residual connections is sufficient. NIAs of the decoder MHCA resulted in the second highest reduction of gIoU and F1-score, and showed a steady decline in regression performance, with a loss of 26%p mgIoU at 50% ablation, while classification performance remained stable until the highest ablation level. This highlights the decoder MHCA’s central role in integrating encoder features over MHSA’s query re-projection function. Although QE ablations resulted in significant regression deterioration, mgIoU only dropped by a maximum of 9%p, contradicting our hypothesis regarding the ranking of model components. The F1-score was less affected with a maximum decrease of  $\approx 5\%$ p, supporting their primary function lies in localization as intended by Carion et al. [27]. Encoder MHSA ablations led to the highest performance drop—39%p in mgIoU and 29%p in F1-score at 50% ablation—contradicting our hypothesis based on the DETR paper by underscoring its essential role in constructing features for both localization and classification. Figure 3 visualizes the results of the block-wise ablations, following the same concept as Fig. 2. With the exception that the x-axis depicts the transformer block in which the 30% ablations were performed. We exclude the results of the decoder MHSA due to negligible effects. NIAs in the encoder MHSA

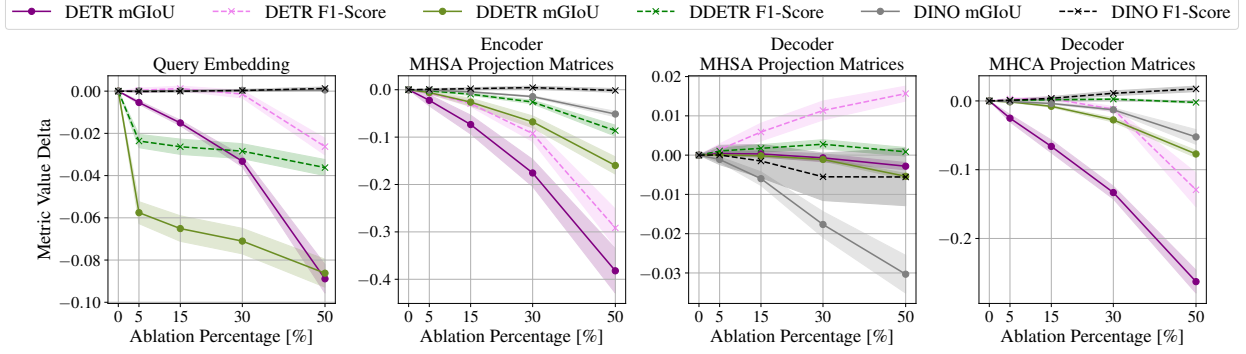


Figure 2: DETR, DDETR and DINO performance differences for increasing ablation percentages in QEs, encoder MHSA, decoder MHSA and decoder MHCA. The shaded areas correspond to the standard deviation. Separate visualizations for each model in Appendix Fig. A2, A3, A4

reveal a steadily decreasing mIoU from block four onward, indicating that substantial feature refinement mostly occurs in the deeper half of the encoder. Classification displays no clear trend, with F1-score fluctuations between 0.44%p and 1.1%p, suggesting that class-discriminative information is redundantly encoded across multiple blocks. Decoder MHCA ablations, unexpectedly, improved classification across all blocks, peaking at block four with +1.3%p F1-score. Regression performance declined steadily up to block five but rebounded at block six, deviating from both our hypothesis and the original DETR findings. This implies that only the final three to four decoder blocks meaningfully contribute to regression, while classification ability may be constrained by training dynamics.

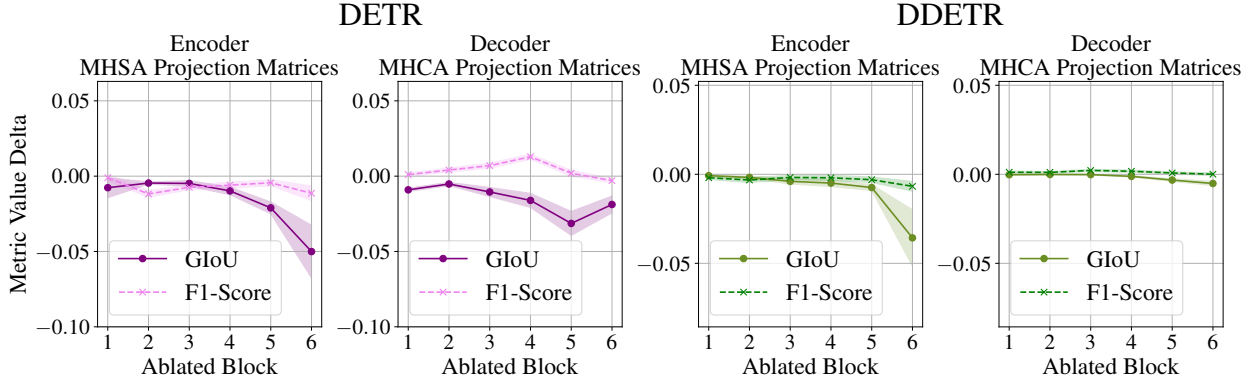


Figure 3: DETR and DDETR performance difference for 30% block-wise ablations in encoder MHSA and decoder MHCA. The shaded areas correspond to the standard deviation.

## 4.2 Deformable Detection Transformer Model (DDETR)

Our hypotheses for the DDETR ablations stem from its two core innovations: multi-scale features and deformable attention. We expect that adopting multi-scale features leads to larger performance losses in both considered metrics, because each ablated value in the projection matrices influences more intermediate results, compared to DETR. This effect is caused by concatenating the 6.5 larger input along the embedding dimension, before multiplying it with the projection matrices. In contrast, deformable attention likely increases resilience to ablation by reducing the likelihood of ablating critical parameters, through reducing the number of attended tokens per head from  $H/32 \times W/32$  (height/width of the input image) to four (single-scale) or sixteen (multi-scale). Given that both the encoder MHSA and decoder MHCA utilize this mechanism, we anticipate a reduced sensitivity in these components. In addition, the larger feature pool created by combining deformable attention with multi-scale inputs may further reduce the ablation effect. It is difficult to predict which of these opposing effects will dominate. The decoder MHSA remains standard, as in DETR, so we anticipate no change in ablation sensitivity. DDETR also increases the number of QEs from 100 to 300 and doubles their embedding size, likely leading to finer-grained representations more susceptible to ablation. The new parameters added by the increased embedding size act as learnable reference points for the first decoder MHCA layer. To isolate

effects, we separate QE and reference point ablations. The performance curves for DDETR’s encoder MHSA closely resemble those of DETR, though the impact is only half as severe. We observe very similar behavior for the decoder MHCA ablations’ effect on regression performance, while classification remains unaffected. With NIA we were able to show that deformable attention’s reduction to the most important tokens can compensate for the disproportionate influence increase of projection matrix values due to multi-scale feature concatenation. Decoder MHSA again has negligible impact, aligning with the expectations. Ablating DDETR’s QEs results in a sharp performance drop of  $\approx 6\%p$  with only 5% ablation, indicating greater sensitivity compared to DETR. This finding aligns with our hypothesis that QEs play a more critical role in DDETR. However, the total performance reduction at 50% ablation is very similar to DETR. Class-wise performance analysis of both models, reveals that the added parameters in DDETR primarily support distinctions among the most frequent 70-80% classes (Appendix fig. A5). Ablating reference points alone results in minimal performance reduction  $\approx 0.1\%$ , revealing that the QEs constitute the major functionality contribution (Appendix fig. A6). The block-wise ablation results presented on the right of figure 3 reveal a more distributed knowledge representation compared to DETR, especially in the decoder. Due to negligible effects, the decoder MHSA results are omitted. Targeting the encoder MHSA demonstrates that the first five blocks contribute little to the overall performance, only the final block causes a notable 3.6%p mIoU decrease, underscoring redundancy in earlier layers. The decoder MHCA is largely unaffected by single-block ablations, reinforcing the observation that deformable attention features facilitate the emergence of resilient representations.

### 4.3 Detection Transformer Model with Improved DeNoising Anchor Boxes (DINO)

Building on the architectural innovations introduced in the DINO paper, we formulate the following hypotheses regarding the impact of dynamic anchors and the "look forward twice" mechanism. Dynamic anchors may reduce the relevance of static content query (embeddings), by providing information tailored to each input image rather than fixed decoder inputs. The "look forward twice" mechanism introduces an additional gradient path by basing prediction boxes  $b_i^{aux}$  used in auxiliary losses on predictions of the previous decoder block  $b_{i-1}$  instead of its own. These boxes are corrected by their own results  $\Delta b_i$ . We hypothesize that this approach improves inter-block consistency in prediction across decoder blocks. Ablating the acpqe has minimal impact, as expected, because dynamic anchors directly transmit positional information from encoder to decoder. This becomes even clearer when we compare the sparsity levels, measured by the percentage of near-zero values (range  $\pm 0.05$ ) in the QEs: DINO shows a sparsity of 58%, compared to just  $\approx 4\%$  in DETR and DDETR. Completely ablating the static content queries shows an increase in mIoU by  $+0.03\%p$  and by  $+1.15\%p$  F1-score, making DINO the top performer across both metrics. This suggests that the ability that emerged from the content queries of DETR and DDETR shifted to the encoder with DINO, making content queries obsolete. To validate this, we retrained DINO under standard mmdetection settings with frozen content queries set to zero. The model trained without learnable content queries achieves 81.08% mIoU and 86.9% F1-score, while the model with learnable content queries obtains 81.63% mIoU and 85.45% F1-score. We also completely ablated the content queries from our self-trained model to ensure that we observe the same behavior as in the mmdetection model, which we did with  $-0.02\%p$  mIoU and  $+2.19\%p$  F1-score. Thus, the content queries seem to assist in the early stages of training, but are largely disregarded later, reflected by their increasing sparsity (67% for our self-trained model). Ablations in encoder MHSA caused only minor decreases in mIoU and F1-score. The decoder’s MHSA exerts a

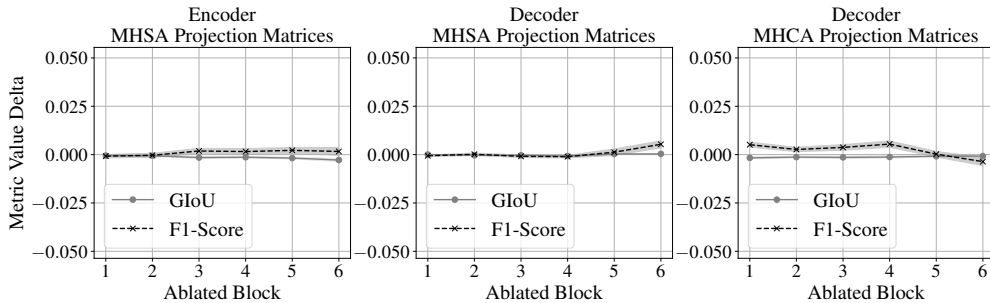


Figure 4: DINO performance difference for 30% block-wise ablations in encoder MHSA and decoder MHCA. The shaded areas correspond to the standard deviation.

greater influence than in DETR and DDETR, due to its processing of dynamic anchors fused with the static queries - though this fusion may hinder convergence, given the latter’s declining relevance as training progresses. Decoder MHCA ablations uniquely led to an increase in classification performance alongside a decrease in regression ability, suggesting a prioritization of localization over classification. This trend mirrors the observed gain in mIoU and accompanied by slight F1-score decline from DDETR to DINO, noted at the beginning of section 4. DINO exhibits

almost no performance degradation when any attention layers are ablated block-wise as visualized in fig. 4. Minor positive changes in F1-score were observed from block three onward, showing that classification benefited slightly from encoder MHSA ablations. The knowledge distribution across decoder blocks led to minor gains in classification and negligible regression loss. DINO’s block-wise ablations indicate that training with the “look forward twice” rule results in the aspired objective - highly distributed knowledge across blocks [45].

## 5 Conclusion and Future Work

We conducted NIA studies on DETR models trained on the COCO dataset, along the guiding question of how specific innovations introduced with DETR, DDETR, and DINO affect the organization of their learned representations. Key components that differentiate DETRs from CNNs and NLP transformers—encoder and decoder MHSA, MHCA projection matrices, and QEs — were systematically ablated at varying levels (5–50%) across all blocks and in a single block setting (30%). To support reproducibility and further exploration, we provide the *DeepDissect* library. We found that the effect of ablations on model performance significantly decreases from DETR over DDETR to DINO. DETR showed to rely heavily on the encoder MHSA and decoder MHCA for regression and classification, while ablations in the QEs only moderately impact regression performance. However, ablating parts of the decoder MHSA has minimal impact on regression and even slightly improve classification, suggesting potential for parameter reduction and inference speed up by directly feeding QEs into the MHCA layer. The combination of multi-scale features with deformable attention in DDETR leads to a reduced effect of ablations in encoder MHCA and decoder MHCA. QEs become significantly more sensitive at 5% ablation percentage, due to overfitting on frequent classes, caused by a parameter increase compared to DETR. The higher selectivity of the deformable attention leads to a concentration of representations important for regression in the last encoder block, where the decoder MHCA has high redundancy over all blocks. DINO’s look forward twice update rule leads to redundant representations for both object detection subtasks that are well distributed across the whole model. This redundancy opens up the possibility for efficiency gains via block reduction while retaining performance. NIAs help to uncover that the direct information transfer from encoder to decoder via dynamic anchor boxes makes content queries obsolete in the fully trained state, as the function they fulfilled in DETR and DDETR emerges in DINO’s encoder. By training DINO without static QEs, we found that they still support in the early stages of training, but become irrelevant as training progresses. In our future work, we aim to expand our ablation experiments to additional components like FFN or the offset sampling and attention weight prediction in deformable attention. Additional experiments with the DDETR variants utilizing refinements (one/two stage) would be interesting to see if they show comparable behavior to DINO, as these use the encoder features to enhance QEs as well. Furthermore, we would like to explore ablation target selection schemes beyond simple randomization and analyze class-level representations using specifically designed datasets in conjunction with NIA studies. Finally, we aim to establish NIAs as a standard tool for improving understanding of the inner workings of deep learning models through our continued refinement of the methodology.

## A Appendix

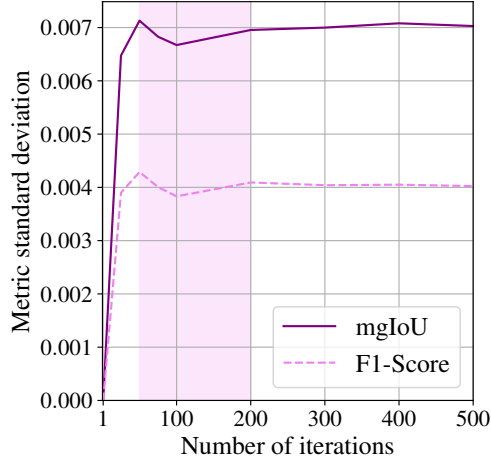


Figure A1: Standard deviation of mIoU and F1-Score for varying numbers of random configuration in query embedding ablations.

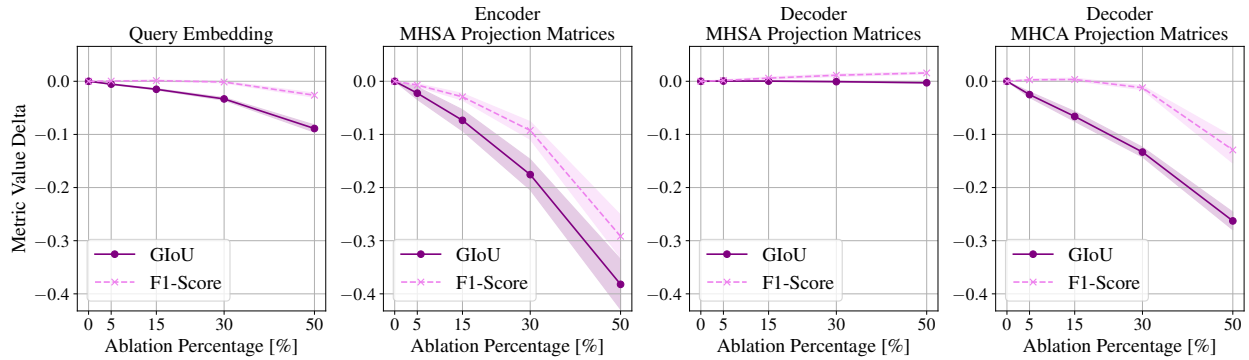


Figure A2: DETR performance differences for increasing ablation percentages in QEs, encoder MHSA, decoder MHSA and decoder MHCA. The shaded areas correspond to the standard deviation.

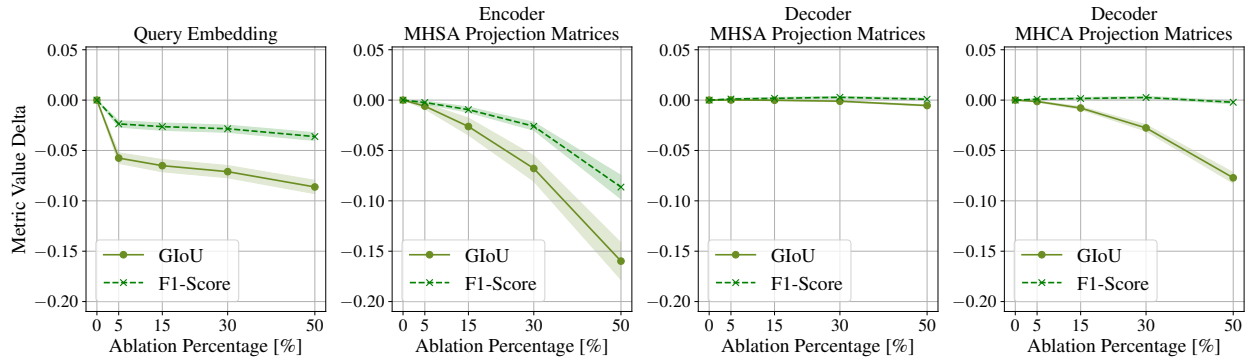


Figure A3: DDETR performance differences for increasing ablation percentages in QEs, encoder MHSA, decoder MHSA and decoder MHCA. The shaded areas correspond to the standard deviation.

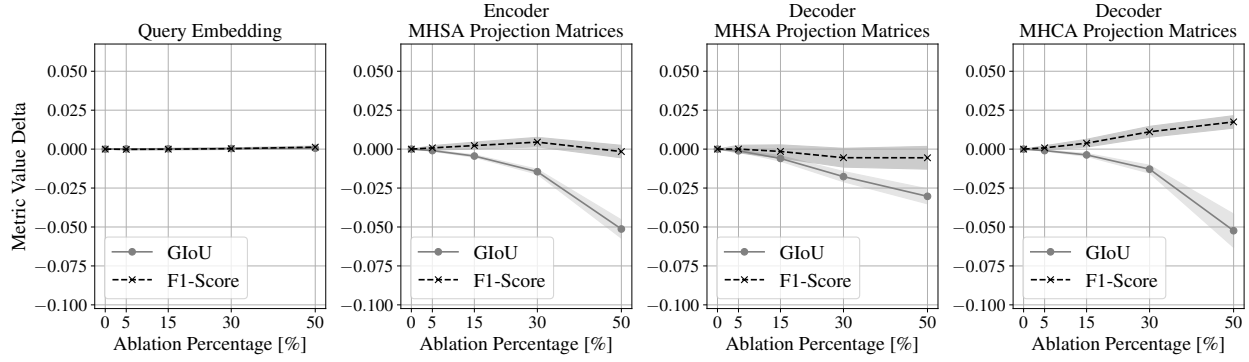


Figure A4: DINO performance differences for increasing ablation percentages in QEs, encoder MHSA, decoder MHSA and decoder MHCA. The shaded areas correspond to the standard deviation.

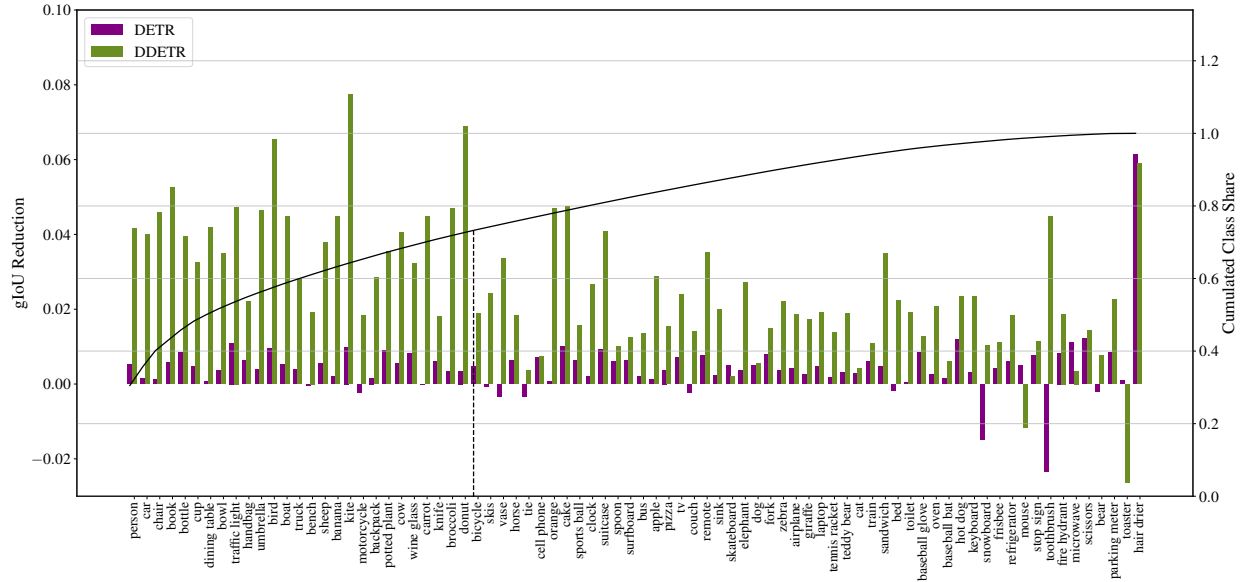


Figure A5: DINO performance differences for increasing ablation percentages in QEs, encoder MHSA, decoder MHSA and decoder MHCA. The shaded areas correspond to the standard deviation.

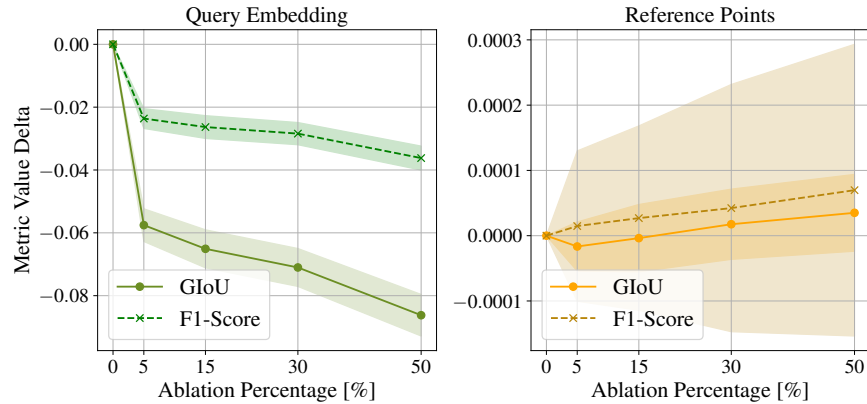


Figure A6: DDETR performance differences for increasing ablation percentages in QEs and reference points. The shaded areas correspond to the standard deviation.

## References

- [1] Ashish Vaswani, Noam Shazeer, Niki Parmar, Jakob Uszkoreit, Llion Jones, Aidan N. Gomez, Lukasz Kaiser, and Illia Polosukhin. Attention is all you need. In *Advances in Neural Information Processing Systems*, volume 30, 2017.
- [2] Alexey Dosovitskiy, Lucas Beyer, Alexander Kolesnikov, Dirk Weissenborn, Xiaohua Zhai, Thomas Unterthiner, Mostafa Dehghani, Matthias Minderer, Georg Heigold, Sylvain Gelly, et al. An image is worth 16x16 words: Transformers for image recognition at scale. *arXiv preprint arXiv:2010.11929*, 2020.
- [3] Ze Liu, Yutong Lin, Yue Cao, Han Hu, Yixuan Wei, Zheng Zhang, Stephen Lin, and Baining Guo. Swin transformer: Hierarchical vision transformer using shifted windows. In *Proceedings of the IEEE/CVF International Conference on Computer Vision*, pages 10012–10022, 2021.
- [4] Jianwei Yang, Chunyuan Li, Pengchuan Zhang, Xiyang Dai, Bin Xiao, Lu Yuan, and Jianfeng Gao. Focal self-attention for local-global interactions in vision transformers, 2022.
- [5] Salman Khan, Muzammal Naseer, Munawar Hayat, Syed Waqas Zamir, Fahad Shahbaz Khan, and Mubarak Shah. Transformers in vision: A survey. *arXiv preprint arXiv:2101.01169*, 2021.
- [6] Nils Hütten, Miguel Alves Gomes, Florian Hölken, Karlo Andricevic, Richard Meyes, and Tobias Meisen. Deep learning for automated visual inspection in manufacturing and maintenance: A survey of open- access papers. *Applied System Innovation*, 7(1):11, 2024.
- [7] Jacob Devlin, Ming-Wei Chang, Kenton Lee, and Kristina Toutanova. Bert: Pre-training of deep bidirectional transformers for language understanding. *arXiv preprint arXiv:1810.04805*, 2018.
- [8] Tom Brown, Benjamin Mann, Nick Ryder, Melanie Subbiah, Jared Kaplan, Prafulla Dhariwal, Arvind Neelakantan, Pranav Shyam, Girish Sastry, Amanda Askell, Sandhini Agarwal, Ariel Herbert-Voss, Gretchen Krueger, Tom Henighan, Rewon Child, Aditya Ramesh, Daniel M. Ziegler, Jeffrey Wu, Clemens Winter, Christopher Hesse, Mark Chen, Eric Sigler, Mateusz Litwin, Scott Gray, Benjamin Chess, Jack Clark, Christopher Berner, Sam McCandlish, Alec Radford, Ilya Sutskever, and Dario Amodei. Language models are few-shot learners. *arXiv preprint arXiv:2005.14165*, 2020.
- [9] Ze Liu, Han Hu, Yutong Lin, Zhuliang Yao, Zhenda Xie, Yixuan Wei, Jia Ning, Yue Cao, Zheng Zhang, Li Dong, et al. Swin transformer v2: Scaling up capacity and resolution. In *Proceedings of the IEEE/CVF Conference on Computer Vision and Pattern Recognition*, pages 12009–12019, 2022.
- [10] Lu Yuan, Dongdong Chen, Yi-Ling Chen, Noel Codella, Xiyang Dai, Jianfeng Gao, Houdong Hu, Xuedong Huang, Boxin Li, Chunyuan Li, Ce Liu, Mengchen Liu, Zicheng Liu, Yumao Lu, Yu Shi, Lijuan Wang, Jianfeng Wang, Bin Xiao, Zhen Xiao, Jianwei Yang, Michael Zeng, Luwei Zhou, and Pengchuan Zhang. Florence: A new foundation model for computer vision, 2021.
- [11] Jianwei Yang, Chunyuan Li, Xiyang Dai, Lu Yuan, and Jianfeng Gao. Focal modulation networks, 2022.
- [12] Wenhai Wang, Jifeng Dai, Zhe Chen, Zhenhang Huang, Zhiqi Li, Xizhou Zhu, Xiaowei Hu, Tong Lu, Lewei Lu, Hongsheng Li, Xiaogang Wang, and Yu Qiao. Internimage: Exploring large-scale vision foundation models with deformable convolutions, 2022.
- [13] Sédrick Stassin, Valentin Corduant, Sidi Ahmed Mahmoudi, and Xavier Siebert. Explainability and evaluation of vision transformers: An in-depth experimental study. *Electronics*, 13(1):175, 2024.
- [14] Moritz Böhle, Jonas Löffler, Christian Pahins, and Kristian Kersting. Holistically explainable vision transformers. *arXiv preprint arXiv:2301.08669*, 2023.
- [15] Rojina Kashefi, Leili Barekatin, Mohammad Sabokrou, and Fatemeh Aghaeipoor. Explainability of vision transformers: A comprehensive review and new perspectives. *arXiv preprint arXiv:2311.06786*, 2023.
- [16] William B. Scoville and Brenda Milner. Loss of recent memory after bilateral hippocampal lesions. *Journal of Neurology, Neurosurgery & Psychiatry*, 20(1):11–21, 1957.
- [17] Edmund T. Rolls. Hippocampo-cortical and cortico-cortical backprojections. *Hippocampus*, 10(4):380–388, 2000.
- [18] Leslie G. Ungerleider and Mortimer Mishkin. Two cortical visual systems. In David J. Ingle, Melvyn A. Goodale, and Richard J. W. Mansfield, editors, *Analysis of Visual Behavior*, pages 549–586. MIT Press, Cambridge, MA, 1982.
- [19] Joseph LeDoux. The emotional brain: The mysterious underpinnings of emotional life. *Simon and Schuster*, 1996.
- [20] Richard Meyes, Melanie Lu, Constantin Waubert de Puiseau, and Tobias Meisen. Ablation studies in artificial neural networks. *arXiv preprint arXiv:1901.08644*, 2019.

- [21] Kai Chen, Jiaqi Wang, Jiangmiao Pang, Yuhang Cao, Yu Xiong, Xiaoxiao Li, Shuyang Sun, Wansen Feng, Ziwei Liu, Jiarui Xu, Zheng Zhang, Dazhi Cheng, Chenchen Zhu, Tianheng Cheng, Qijie Zhao, Buyu Li, Xin Lu, Rui Zhu, Yue Wu, Jifeng Dai, Jingdong Wang, Jianping Shi, Wanli Ouyang, Chen Change Loy, and Dahua Lin. MMDetection: Open mmlab detection toolbox and benchmark. *arXiv preprint arXiv:1906.07155*, 2019.
- [22] Tsung-Yi Lin, Michael Maire, Serge Belongie, James Hays, Pietro Perona, Deva Ramanan, Piotr Dollár, and C Lawrence Zitnick. Microsoft coco: Common objects in context, 2014.
- [23] Allen Newell. A tutorial on speech understanding systems. *Speech Recognition: Invited Papers Presented at the 1974 IEEE Symposium*, 1975:3, 1974.
- [24] Saining Xie, Ross Girshick, Piotr Dollár, Zhuowen Tu, and Kaiming He. Aggregated residual transformations for deep neural networks, 2017.
- [25] Shaoqing Ren, Kaiming He, Ross Girshick, and Jian Sun. Faster r-cnn: Towards real-time object detection with region proposal networks, 2015.
- [26] Tsung-Yi Lin, Piotr Dollár, Ross Girshick, Kaiming He, Bharath Hariharan, and Serge Belongie. Feature pyramid networks for object detection, 2017.
- [27] Nicolas Carion, Francisco Massa, Gabriel Synnaeve, Nicolas Usunier, Alexander Kirillov, and Sergey Zagoruyko. End-to-end object detection with transformers, 2020.
- [28] Ross Girshick, Jeff Donahue, Trevor Darrell, and Jitendra Malik. Rich feature hierarchies for accurate object detection and semantic segmentation, 2013.
- [29] Isha Hameed, Samuel Sharpe, Daniel Barcklow, Justin Au-Yeung, Sahil Verma, Jocelyn Huang, Brian Barr, and C. Bayan Bruss. Based-xai: Breaking ablation studies down for explainable artificial intelligence, 2022.
- [30] Y. Vishnusai, Tejas R. Kulakarni, and K. Sowmya Nag. Ablation of artificial neural networks. In Jennifer S. Raj, Abul Bashar, and S. R. Jino Ramson, editors, *Innovative Data Communication Technologies and Application*, volume 46 of *Lecture Notes on Data Engineering and Communications Technologies*, pages 453–460. Springer International Publishing, Cham, 2020.
- [31] Peter E. Lillian, Richard Meyes, and Tobias Meisen. Ablations on a robot’s brain: Neural networks under a knife. *Institute of Information Management in Mechanical Engineering, RWTH Aachen University*, 2019.
- [32] Ramprasaath R. Selvaraju, Michael Cogswell, Abhishek Das, Ramakrishna Vedantam, Devi Parikh, and Dhruv Batra. Grad-cam: Visual explanations from deep networks via gradient-based localization. In *2017 IEEE International Conference on Computer Vision (ICCV)*, pages 618–626, 2017.
- [33] Richard Meyes, Nils Hütten, and Tobias Meisen. Transparent and interpretable failure prediction of sensor time series data with convolutional neural networks. *Procedia CIRP*, 2021.
- [34] Elias Frantar and Dan Alistarh. Sparsegpt: Massive language models can be accurately pruned in one-shot. *arXiv preprint arXiv:2301.00774v3*, 2023.
- [35] Xin Men, Mingyu Xu, Qingyu Zhang, Bingning Wang, Hongyu Lin, Yaojie Lu, Xianpei Han, and Weipeng Chen. Shortgpt: Layers in large language models are more redundant than you expect. *arXiv preprint arXiv:2403.03853v3*, 2024.
- [36] Mingjie Sun, Zhuang Liu, Anna Bair, and J. Zico Kolter. A simple and effective pruning approach for large language models. In *Proceedings of the International Conference on Learning Representations (ICLR)*, 2024.
- [37] Dachuan Shi, Chaofan Tao, Ying Jin, Zhendong Yang, Chun Yuan, and Jiaqi Wang. Upop: Unified and progressive pruning for compressing vision-language transformers. In *Proceedings of the 40th International Conference on Machine Learning (ICML)*, 2023.
- [38] Bo-Kyeong Kim, Geonmin Kim, Tae-Ho Kim, Thibault Castells, Shinkook Choi, Junho Shin, and Hyoung-Kyu Song. Shortened llama: Depth pruning for large language models with comparison of retraining methods. *arXiv preprint arXiv:2301.13741v3*, 2024.
- [39] Fang Yu, Kun Huang, Meng Wang, Yuan Cheng, Wei Chu, and Li Cui. Width & depth pruning for vision transformers. *Proceedings of the AAAI Conference on Artificial Intelligence*, 36(3):3143–3151, 2022.
- [40] Lu Yu and Wei Xiang. X-pruner: explainable pruning for vision transformers. In *2023 IEEE/CVF Conference on Computer Vision and Pattern Recognition (CVPR)*, pages 24355–24363, 2023.
- [41] Yifei Liu, Mathias Gehrig, Nico Messikommer, Marco Cannici, and Davide Scaramuzza. Revisiting Token Pruning for Object Detection and Instance Segmentation . In *2024 IEEE/CVF Winter Conference on Applications of Computer Vision (WACV)*, pages 2646–2656, Los Alamitos, CA, USA, January 2024. IEEE Computer Society.

- [42] Hailin Su, Haijiang Sun, and Yongxian Zhao. Efficient pruning of detection transformer in remote sensing using ant colony evolutionary pruning. *Applied Sciences*, 15(1):200, 2025.
- [43] Huaiyuan Sun, Shuili Zhang, Xve Tian, and Yuanyuan Zou. Pruning detr: efficient end-to-end object detection with sparse structured pruning. *Signal, Image and Video Processing*, 18(1):129–135, 2024.
- [44] Xizhou Zhu, Weijie Su, Lewei Lu, Bin Li, Xiaogang Wang, and Jifeng Dai. Deformable detr: Deformable transformers for end-to-end object detection, 2020.
- [45] Hao Zhang, Feng Li, Shilong Liu, Lei Zhang, Hang Su, Jun Zhu, Lionel Ni, and Heung-Yeung Shum. DINO: DETR with improved denoising anchor boxes for end-to-end object detection. In *The Eleventh International Conference on Learning Representations*, 2023.
- [46] H. Rezatofighi, N. Tsoi, J. Gwak, A. Sadeghian, I. Reid, and S. Savarese. Generalized intersection over union: A metric and a loss for bounding box regression. In *2019 IEEE/CVF Conference on Computer Vision and Pattern Recognition (CVPR)*, pages 658–666, Los Alamitos, CA, USA, jun 2019. IEEE Computer Society.